

# Graphene coatings: An efficient protection from oxidation

M. Topsakal,<sup>1,2</sup> H. Şahin,<sup>1,2</sup> and S. Ciraci<sup>1,2,3,\*</sup>

<sup>1</sup>UNAM-National Nanotechnology Research Center, Bilkent University, 06800 Ankara, Turkey

<sup>2</sup>Institute of Materials Science and Nanotechnology, Bilkent University, 06800 Ankara, Turkey

<sup>3</sup>Department of Physics, Bilkent University, 06800 Ankara, Turkey

(Dated: November 1, 2018)

We demonstrate that graphene coating can provide an efficient protection from oxidation by posing a high energy barrier to the path of oxygen atom, which could have penetrated from the top of graphene to the reactive surface underneath. Graphene bilayer, which blocks the diffusion of oxygen with a relatively higher energy barrier provides even better protection from oxidation. While an oxygen molecule is weakly bound to bare graphene surface and hence becomes rather inactive, it can easily dissociate into two oxygen atoms adsorbed to low coordinated carbon atoms at the edges of a vacancy. For these oxygen atoms the oxidation barrier is reduced and hence the protection from oxidation provided by graphene coatings is weakened. Our predictions obtained from the state of the art first-principles calculations of electronic structure, phonon density of states and reaction path will unravel how a graphene can be used as a corrosion resistant coating and guide further studies aiming at developing more efficient nanocoatings.

PACS numbers: 81.16.Pr, 68.65.Pq, 66.30.Pa, 81.05.ue

## I. INTRODUCTION

The reaction of material surfaces with oxygen and controlling damages from corrosion have been the subject of intensive research for decades. While protective macroscale coatings give rise to the modification of the sizes and some other physical properties of reactive surfaces, progress made to date has revealed several advantages of nanoscale coatings in protection from corrosion and wear.

The earliest efforts of protection from oxidation using carbon based materials were devoted to the carbon deposition on metal surfaces. It was reported that Ni and Co surfaces can be covered by carbon deposition at high temperatures.<sup>1</sup> It was shown that the (111) surfaces of the Ni single crystals can be covered by monolayer carbon as a result of carbon segregation through the metal surface.<sup>2</sup> Soon after, the surface segregation behavior of carbon from dilute solid solutions on Pt(100), Pt(111), Pd(100), Pd(111) and Co(0001) surfaces was investigated.<sup>3</sup> Interestingly, much earlier it was argued that had the segregated carbon layer can be in the form of monolayer honeycomb structure like graphene.<sup>4</sup>

Graphene,<sup>5</sup> being not only the thinnest ever but also the strongest material, has, in fact, the potential for nano-coating applications. When sticks to or grown on various surfaces, graphene adds only negligible thickness to the size of the underlying sample and forms an electrically and thermally conductive coating on it. Moreover, graphene has exceptional mechanical, thermal and chemical stability. Various synthesis techniques of graphene covered metal surfaces and their electronic and structural properties have been reviewed by Winterlin *et al.*<sup>6</sup> and Mattevi *et al.*<sup>7</sup> Advances in the techniques of graphene synthesis have initiated the studies on graphene coating. Experimentally, Dedkov *et al.*<sup>8</sup> studied the oxygen protection of Fe intercalated Ni surface and bare Ni films.

Borca *et al.*<sup>9</sup> have experimentally demonstrated that the periodically rippled structure of graphene can be grown on Ru(0001) surface and it serves as a perfect coating material against oxidation. Much recently, Gadipelli *et al.*<sup>10</sup> reported the formation of large-scale graphene monolayers on Cu surface, which is well-protected from the oxidation. Also the graphene coatings on Cu, Cu/Ni alloy, Pt and Ir surfaces have been exploited.<sup>11–13</sup> XPS and SEM images presented evidences that Cu and Cu/Ni surfaces can be protected from oxidation through graphene coating.<sup>11</sup> However, despite these recent progresses, very little is known how and why graphene layer constitutes a protective coating on reactive surfaces and what are its limitations.

In this study we show that graphene can easily be oxidized by oxygen atoms which form strong chemical bonds on its surface. Despite that the graphene coating can protect solid surfaces from oxidation by posing a high energy barrier to any adsorbed oxygen atom diffusing from the top of graphene to the interface between graphene and the reactive surface underneath. Because of this barrier perpendicular diffusivity of oxygen atom is practically zero as compared to its lateral diffusivity. Although an oxygen molecule is weakly bound to graphene and does not have any direct role in the oxidation, it can be indirectly involved by dissociating into two atomic oxygens. These oxygen atoms form relatively stronger chemical bonds with twofold coordinated carbons but encounter much lower oxidation barrier when diffuse towards the reactive surface. Poor protection from oxidation at defect sites can be circumvented by multilayer graphene coating.

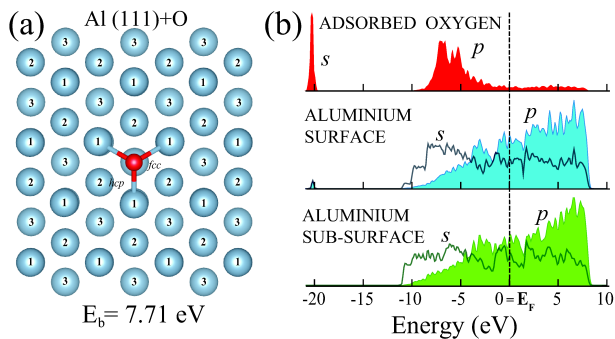


FIG. 1: (a) Atomic configuration of an oxygen atom adsorbed to Al(111) surface. Oxygen and Al atoms are illustrated by small-red and large-blue balls with numerals indicating their layer numbers from the top. (b) Density of states (DOS) projected to  $s$ - and  $p$ -orbitals of adsorbed O, surface and sub-surface layers of Al(111) slab.

## II. METHOD

Our study proceeds in three complementary and sequential steps: (i) In the first step we examine the interaction of  $O_2$  and O atoms with a bare reactive metal surface and with a bare pristine graphene, where important features are discovered. (ii) Second step deals with the sticking of graphene to a flat, clean surface, which is vulnerable to oxidation. (iii) In the third step, we show how graphene coating hinders oxygen atoms from diffusion towards the protected surface. Our results are obtained by performing first-principles, spin-polarized calculations within Density Functional Theory using VASP package.<sup>14,15</sup> We used Generalized Gradient Approximation<sup>16</sup> including Van der Waals (vdW) correction<sup>17</sup>, PAW potentials<sup>18</sup> and a plane wave basis set with the kinetic energy cutoff of 500 eV. To minimize the coupling between adsorbed atoms or molecules, the binding energies and reaction paths are calculated using (4x4) or (6x6) supercells. For the coated surfaces a grid of 25x25x1  $k$ -points is used. The convergence criterion of self consistent calculations for ionic relaxations is taken  $10^{-5}$  eV between two consecutive steps. By using the conjugate gradient method, atomic positions and lattice constants are optimized until the atomic forces are less than 0.05 eV/Å. The energetics of various paths of O or  $O_2$  are calculated by forcing them to pass through the graphene layer from above to below. The amount of displacement is identified as *indentation* in the figures. The paths of minimum energy barrier are determined by relaxing carbon atoms of graphene, as well as lateral  $x$ - and  $y$ -coordinates of O or  $O_2$  at each step of indentation corresponding to a fixed  $z$ -coordinate. In some cases, the energy barriers associated with specific and well-determined paths are also examined, where  $O_2$  and O are forced to follow these paths, but the rest of atoms are relaxed. The maximum number of atoms treated in our calculations is 129, which occurred in the determination of energy bar-

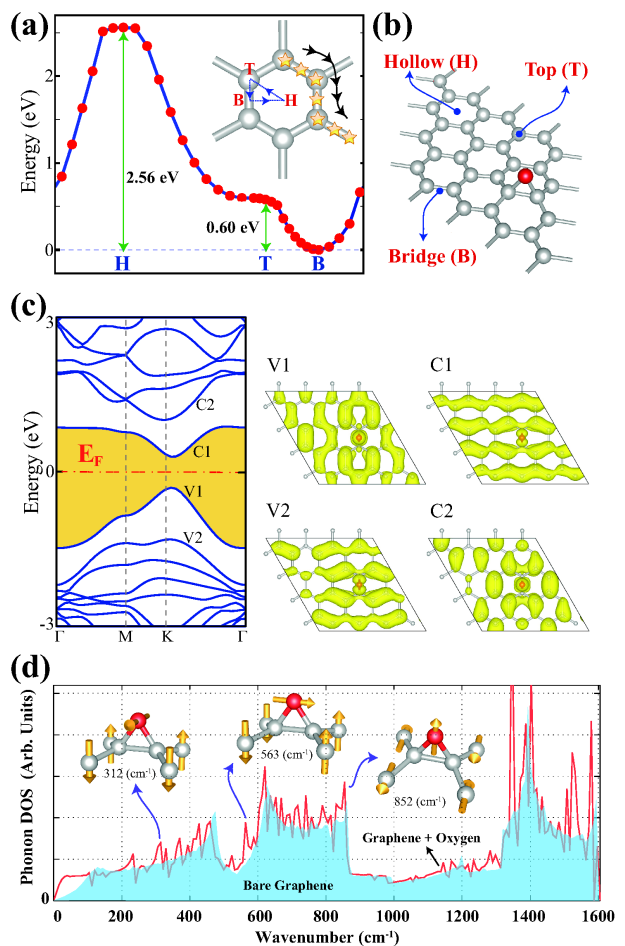


FIG. 2: (a) Variation of the energy of adsorbed oxygen atom along T(top)-H(hollow)-B(bridge) site directions of a hexagon showing that the B-site is energetically most favorable. Stars indicate favorable path for the diffusion of oxygen atom on the graphene surface. (b) Atomic configuration for an oxygen atom adsorbed at the bridge site on a (4x4) supercell of graphene consisting of 32 carbon atoms. (c) Electronic energy band structure together with the charge densities of specific conduction and valence band states. (d) Calculated density of phonon modes of a pristine graphene (shaded area) and those of oxygen adsorbed to the bridge site of the (4x4) supercell of graphene (red line). Relevant localized phonon modes are indicated by insets.

riers associated with the coating of Al(111) surface by graphene bilayer.

## III. OXIDATION OF AL SURFACE AND GRAPHENE

Since we are not concerned with sample specific details of oxidation behaviors of the protected surfaces, Al(111) surface is taken here only as a prototype metal surface vulnerable to oxidation when exposed to atmosphere, but is protected by placing a graphene sheet between its surface and atmosphere. Al(111) surface alone is repre-

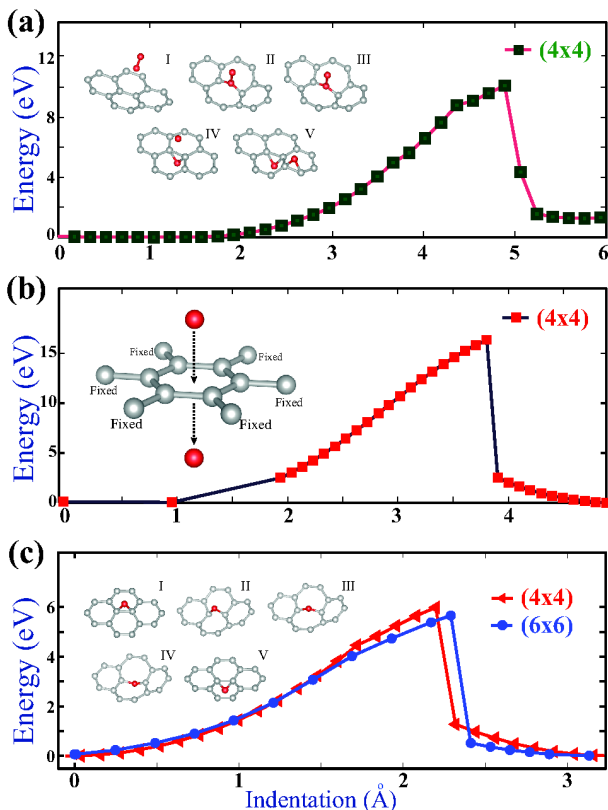


FIG. 3: Calculation of energy barriers of  $O_2$  and  $O$  passing from the top to the bottom side of a suspended graphene along various paths. (a)  $O_2$ , which is forced to pass from the top to bottom side of graphene following a fixed vertical line through the hole at the center of a hexagon. (b) The energy barrier for  $O$  atom along the same path as (a). (c) The path of the minimum energy barrier for an  $O$  atom, which is initially adsorbed at the bridge site above the graphene plane is forced to pass to the bottom side. Positions of  $C$  atoms, as well as the lateral  $x$ - and  $y$ -coordinates of  $O$  are optimized for each value of indentation.

sented by a 4-layer Al(111) slab as described in Fig. 1. It has metallic and nonmagnetic ground state, and its states at the Fermi level ( $E_F$ ) are composed of mainly  $3p_{xy}$ - and partially  $3s$ -orbitals of Al atoms. The work function for this slab is calculated to be 4.06 eV, which is comparable to the value of 4.24 eV measured experimentally<sup>19</sup> for Al(111) surface. We calculate that an oxygen atom is strongly bound to the Al(111) surface with 7.71 eV binding energy at the fcc site and 7.24 eV at the hcp site. Fig. 1 (b) presents the densities of electronic states projected to adsorbate  $O$ , surface and subsurface layers of Al(111) slab. Apparently,  $2p$ -orbitals of adsorbed  $O$  mix with the  $3p$  and  $3s$ -orbitals of Al substrate in a wide energy range to form a strong bond. Oxygen molecule by itself interact strongly with Al(111) surface; it dissociates into atomic oxygens which, in turn, are adsorbed at fcc and hcp sites.

Bare graphene can also be easily oxidized, whereby oxygen atoms are adsorbed at the bridge site positions above any C-C bond of graphene and become negatively

charged. Our calculations using Bader analysis<sup>20</sup> estimates an excess charge of 0.79 electrons at adsorbed  $O$  atom. The binding energy is calculated to be 2.72 eV at the bridge site, hence  $O$  atoms at the T(top)- or H(hollow)- (i.e. center of hexagon) site in Fig. 2 (a) move favorably to the B(bridge)-site. Figure 2 (c) presents the electronic energy band structure corresponding to an  $O$  atom adsorbed to a bridge site of a (4x4) supercell of graphene and the charge density distributions of specific conduction and valence band states. Upon oxidation the linearly crossing  $\pi$  and  $\pi^*$  states of semimetallic bare graphene are modified and opened a band gap of 0.58 eV. This explains why domains of dark (metallic) graphene surface becomes reflecting (insulator) upon oxidation.<sup>21</sup> Reversible oxidation-deoxidation of graphene through heating or charging has been pointed out as potential electronic device application.<sup>21,22</sup> Reversibility is a strong evidence that graphene surface remain chemically stable in the course of oxidation-deoxidation; neither bond breaking nor modification of honeycomb structure does occur. However, the situation is dramatically different for several other surfaces, such as Si, Fe, Te, Al, Cu etc, where the chemical stability is destroyed upon oxidation.<sup>11,23-25</sup> Figure 2 (d) shows the density of phonon modes (DOS) of a pristine graphene and that of oxygen adsorbed to the bridge site of the (4x4) supercell of graphene, which are calculated from the first principles.<sup>26</sup> As seen, adsorbed oxygen atom gives rise to several localized phonon modes, which will be used in estimating the characterized frequency and the diffusivity thereof.

In contrast to oxygen atom, an oxygen molecule has a weak binding with graphene. We calculated its binding energy to be 115 meV, and magnetic moment 1.90  $\mu_B$ , slightly smaller than the magnetic moment of free  $O_2$ . Hence, an  $O_2$  molecule with such a weak binding energy to bare graphene cannot have any significant effect on the oxidation of the protected surface, though the situation can be different for the defected graphene as we will show later. On the other hand, a free  $O$  atom approaching another  $O$  atom already adsorbed on graphene forms a strong bond with the latter and releases  $\sim 4.13$  eV energy in this exothermic process. Eventually an  $O_2$  molecule is formed thereof. This may explain why deoxidation of graphene is provided easily<sup>21</sup> by the STM tip at 100° C at close proximity of oxidized graphene surface, despite the strong binding energy of  $O$  atom. Note that two adsorbed  $O$  at close proximity can also form an  $O_2$  molecule by releasing an energy of 1.60 eV, if they can overcome an energy barrier.

#### IV. PROTECTION OF AL(111) SURFACE BY GRAPHENE COATING

Next we explore the protection of a reactive surface, such as Al(111) by sticking or growing graphene on it. Sticking of graphene on various metals surfaces including

Al(111) surface has been studied earlier.<sup>27</sup> Even though Al(111) surface are not in registry with graphene honeycomb structure and has hexagonal lattice constants  $\sim 10\%$  larger than those of graphene, sticking of graphene on this surface can be achieved. In order to present an estimation value for the adsorption energy of graphene to Al(111) surface one has to compress Al(111) slab laterally and expand graphene lattice in order to achieve the registry for the optimization of final structures using periodic boundary condition. Despite the strain energy spent to obtain the lattice registry, the sticking occurs with a significant binding energy of 2.67 eV per (4x4) supercell or ( $\sim 166$  meV per cell). The sticking of graphene patches to the Al(111) surface in random orientation is a complex and stochastic process, and can even lead to the formation of bubbles, since low coordinated edge atoms have stronger binding with Al(111) surface. Even if the average binding energy per carbon atom is small, it would require significant energy to peel off the strong but flexible graphene layer from the surface.

If graphene patches are placed randomly on Al(111), they may not be severely strained to maintain the lattice registry. Therefore, we rather consider unstrained graphene and compensate the lattice misfit by laterally compressing Al(111) slab. This way we achieve the lattice registry to be able to use the periodic boundary conditions. Under these circumstances, the adsorption energy of graphene to this compressed Al(111) slab, which is calculated to be 2.38 eV per (4x4) super cell (or  $\sim 148$  meV per cell) is not significantly affected. Additionally, the binding energy of O atom to the compressed Al(111) surface (7.15 eV) is still very high. Thus, despite the compression dictated by the periodic boundary conditions, the compressed Al(111) slab is still sufficiently reactive to mimic a surface to be protected by graphene coating.

### A. Diffusion of O<sub>2</sub> and O through a suspended graphene

Now we address the main issue pertaining to how a graphene coating, which by itself is also vulnerable to oxidation can protect a reactive metal surface. To clarify the mechanism of protection from oxidation we first examine how an O<sub>2</sub> molecule or O atom can pass from one side of bare and suspended graphene to the other side. The energetics and energy barriers involved in the course of these processes are calculated in a (4x4) supercell of bare graphene with specific carbon atoms are fixed to prevent the suspended layer from displacement. Here we consider first the fixed vertical path passing through the hole at the center of hexagons (as a seemingly possible diffusion path) and calculate the involved energy barrier when O<sub>2</sub> molecule or O atom are forced to follow this path as summarized in Fig. 3 (a) and (b). An oxygen molecule following this vertical path needs to overcome a barrier of 10.12 eV in Fig. 3 (a). However, once O<sub>2</sub> overcome this barrier, it dissociates into two O atoms;

one O adsorbed above, the other adsorbed below at the bridge sites. Apparently, graphene acts as a membrane, that blocks the passage of O<sub>2</sub>. If an O atom were forced to pass from the top to the bottom side along this fixed vertical path, the energy barrier would be even higher, i.e. 16.34 eV in Fig. 3 (b). This fixed vertical path is not a possible diffusion path with minimum energy barrier, since there are reaction paths with smaller energy barriers as explained below.

The path shown in Fig. 3 (c) starts from the adsorbed oxygen atom at the bridge site at the top side, i.e. the minimum energy configuration of O atom adsorbed on pristine graphene. At each stage of indentation, carbon atoms, as well as  $x$ - and  $y$ -lateral coordinates of O atom are optimized to minimize the energy. As seen from the snapshots of atomic configuration corresponding to various stages, the passage of O takes place around the same bridge bond, whereby O atom switches from the top to the bottom side of graphene by gradually flattening C-O-C bridge bond. The energy barrier to be overcome by an O atom to pass from the top to the bottom side is calculated to be  $Q = 5.98$  eV. To reveal whether the (4x4) supercell may impose constraints on the calculated energy barrier, we calculated the barrier in a relatively larger, (6x6) graphene supercell to be  $Q = 5.65$  eV. The calculated energy barrier is not affected from the size of the supercell and is high enough to block the diffusion and hence to hinder oxidation of the surface underneath. This path is identified as the path of minimum energy barrier for O atom passing from the top to bottom of bare suspended graphene.

### B. Graphene Coating of Al(111)

In the presence of the Al(111) slab underneath the protective graphene coating, we elaborate and further optimize the reaction path in Fig. 3 (c) as the most likely pathway of oxidation. The variation of the energy of an O atom moving along the reaction path of minimum barrier is shown in Fig. 4 (a). The energy barrier along this reaction path is  $Q_{ox} \sim 5.93$  eV and occurs as O is switching from the top side to the bottom side of graphene. Once the diffusing O atom overcomes this barrier, it goes to Al(111) surface via the bridge site below without almost any barrier and oxidizes the metal surface. This energy barrier  $Q_{ox}$  is rather high and hence the protection of graphene against oxidation appears to be very efficient. The significance of high  $Q_{ox}$  can be deduced by comparing the diffusivity of O moving on graphene surface  $D_{\parallel}$  with that of O atom penetrating the graphene coating to oxidize the Al(111) surface,  $D_{\perp}$ .  $D_{\parallel} = a^2 \nu e^{Q/k_B T}$  can be estimated in terms of the energy barrier  $Q = 0.60$  eV in Fig. 2 (a), lattice constant  $a = 1.43$  Å and the characteristic vibration frequency extracted from the calculated localized phonon modes of O in Fig. 2 (d) to be  $\nu \cong 22$  THz. Accordingly, the diffusivity of O penetrating the graphene coating is estimated to be  $D_{\perp} = D_{\parallel} \times 10^{-87}$ ,

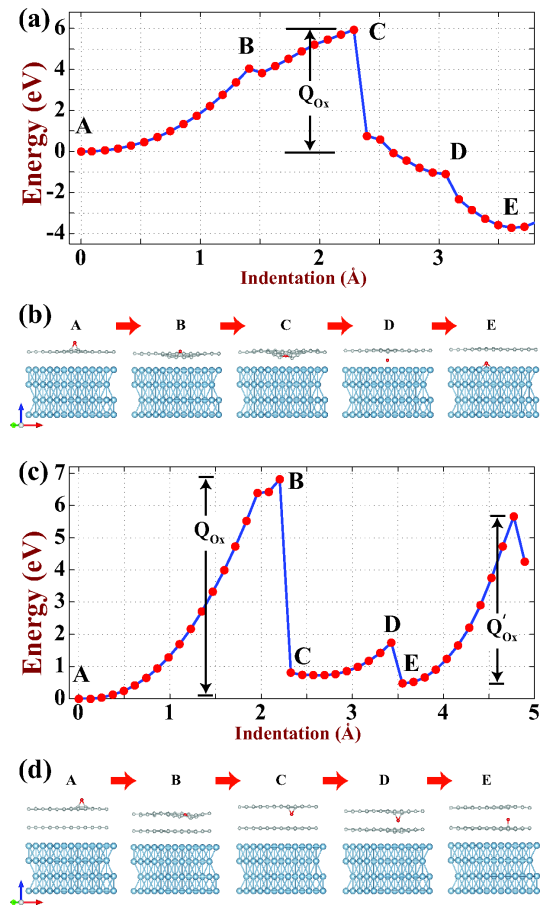


FIG. 4: (a) Variation of the total energy for an O atom (red ball) passing (indenting) from the top side of single graphene layer to its bottom side and eventually adsorbing to Al(111) surface (blue balls) underneath. O atom follows the path of minimum energy barrier ( $Q_{ox}=5.93$  eV). (b) Snapshots of the atomic configurations corresponding to various stages between the initial stage A stating from the bridge site of graphene and final stage E ending with the adsorption of O atom on Al(111). (c) Protection of Al(111) surface from oxidation by a graphene bilayer and the variation of energy for an O atom penetrating from the top side of the outermost graphene layer and eventually adsorbing to Al(111). Highest barrier to be overcome by a diffusing O atom is  $Q_{ox}=6.81$  eV along the the path to reach to Al(111) surface. (d) Atomic configurations of various stages the case of (c).

which is really negligible.

### C. Bilayer Graphene Coating of Al(111)

The effectiveness of the protection against oxidation can be further increased by coating with graphene bilayer. In Fig. 4 (c) the variation of energy of diffusing O atom from outermost graphene bilayer to the metal surface via second graphene layer following the minimum energy reaction path is shown. Apparently, the oxidation barrier is increased by 0.88 eV due to the coating

by graphene bilayer. Snapshots of relevant stages in the course of diffusion of O starting above the first graphene layer through the second graphene layer and eventually ending at the surface of Al(111) surface are also indicated in Fig. 4 (d). While the oxidation barrier  $Q_{ox}=6.81$  eV occurs when the diffusing O switches from the top to the bottom side of first graphene layer, there are additional barriers blocking the diffusion of O atoms. For example, the energy barriers for switching from the bottom bridge site of first layer graphene to the top bridge site of second graphene layer is  $\sim 1$  eV. If this small barrier is overcome, the adsorbed O atom becomes attached to the second graphene layer and is still separated from reactive surface. To proceed with diffusion to reach the Al(111) surface one follows similar course as in Fig. 4 (a). Starting from the stage E, an O atom diffuses from the bridge site above the second graphene layer to the Al(111) surface by overcoming an energy barrier of  $Q'_{ox}=5.20$  eV and oxidizes the metal surface.

Clearly, the coating of reactive surfaces by sheets comprising more than two layers of graphene will further increase the effectiveness of protection. Sequential barriers posed at each graphene layer increase the chance that the diffusing O can be trapped between any two barriers. On the other hand, the size of the protected sample will be modified by each additional graphene layer adding  $\sim 3$  distance between O and Al surface, even if this increase of the thickness may be considered negligible. Protection by graphene sheets comprising a few layers are expected to be effective also to suppress the effects of any local heating or energy transfer to the outermost graphene. For example, as pointed out at the beginning a free oxygen at the close proximity of an adsorbed oxygen on graphene can form  $O_2$ , whereby an energy of  $\sim 4.13$  eV is released. When deposited to the graphene, this energy may create a local, nonequilibrium phonon distribution, which was shown to dissipate within picoseconds.<sup>28,29</sup> Such a short time interval is enough to accommodate several jumps of atoms. Hence a local heating due to a chemical process may promote the diffusion of other adsorbed oxygen atoms from the protective coating towards the reactive surface. Under these circumstances while single layer graphene coating fails to hinder oxidation, multi-layer graphene coating can block the diffusing hot oxygen atoms.

### D. Vacancy Effect

The above arguments related with the protection against oxidation relies on the fact that graphene coating is continuous and defect free. If coating consists of graphene patches, reactive surfaces cannot be covered at the zones between patches, where they become directly exposed to atomic oxygens.<sup>11</sup> The holes or vacancies<sup>30,31</sup> of graphene are also spots, where oxygen atoms would penetrate the metal surface without or relatively smaller energy barrier. In fact, the etching of graphite following

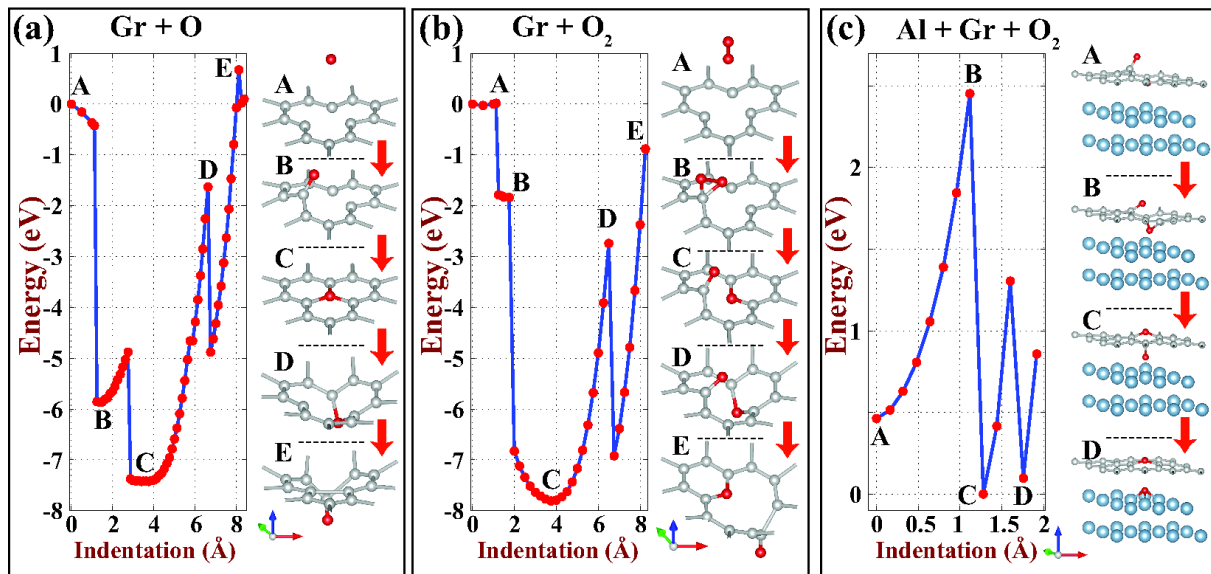


FIG. 5: (a) Evolutions of energetics and atomic structure with the indentation of the oxygen atom, which is initially adsorbed at the edge of a single vacancy. (b) Evolutions of energetics and atomic structure of two oxygen atoms resulting from the dissociation of  $O_2$  molecule at the edge of a single vacancy and the indentation of one of oxygen atoms from the top to the bottom site of a suspended graphene. (c) The diffusion of one of adsorbed oxygen atoms in (b) towards the Al(111) surface resulting in its oxidation. Red, gray and blue balls indicate, respectively O, C and Al atoms.

the dissociation of  $O_2$  by producing CO and  $CO_2$  have been pointed out.<sup>32,33</sup> Here we consider the penetration of oxygen atom near a vacancy in graphene. Three important features of our work are schematically summarized in Fig. 5. An oxygen atom can favorably bound to carbon atoms at the edge of a single vacancy in Fig. 5 (a). The ground state is exothermic and releases 7.65 eV, whereby O atom substitutes the vacant carbon atom. In Fig. 5 (b) an  $O_2$  molecule can dissociate in two O atoms at the close proximity of a vacancy in graphene. Subsequently, while one O atom is attached to one of three twofold coordinated carbon atoms at the edge of the vacancy, the other one bridges between the remaining two and hence completes the hexagon. In this exothermic process 7.83 eV energy is released in addition to the energy spent in dissociation process. This shows that vacancies of graphene are active sites to catalyze the dissociation of  $O_2$  molecules. Fig. 5 (c) shows that the barrier in the diffusion of a specific O atom adsorbed at the edge of a vacancy is dramatically lowered ( $Q_{ox} \sim 2$  eV) and hence the protection from oxidation is weakened. Such a situation shall occur at the grain boundaries and holes of graphene and confirms the experiment<sup>11</sup> that defects or discontinuities in covering a reactive surface by graphene may result in the weakening of the oxidation protection. Similar processes have been also confirmed at the edges of relatively larger holes. This serious limitation caused

by defects can be avoided by multilayer coatings.

## V. CONCLUSIONS

In conclusion, we demonstrated that continuous coating of pristine graphene on reactive surfaces can provide for an excellent protection from oxidation of reactive surfaces at nanoscale. The binding of oxygen atom at low coordinated carbon atoms is rather high, but their barrier to penetrate to the reactive surface under graphene is low. Therefore discontinuities in graphene coating or defects, such as vacancies or holes weaken the protection from oxidation by creating spots of low oxidation barrier. This limitation can be circumvented by coating of bilayer or preferably graphene sheets comprising a few graphene layers, which provides even more effective protection. At macroscale, our results suggests that graphene additives can improve the strength of antioxidant paints. Graphene coating, which is thin at the atomic scale can also serve as a natural barrier between environment and solid surfaces of other elements.

This work is supported by TUBITAK through Grant No:108T234. All the computational resources have been provided by TUBITAK ULAKBIM, High Performance and Grid Computing Center (TR-Grid e-Infrastructure). S. C. acknowledges the partial support of TUBA, Academy of Science of Turkey.

\* Electronic address: ciraci@fen.bilkent.edu.tr

<sup>1</sup> F. J. Derbyshire, A. E. B. Presland, and D. L. Trimm,

- Carbon **13**, 111 (1975).
- <sup>2</sup> M. Eizenberg and J.M. Blakely, Surface Sci. **82**, 228 (1979).
  - <sup>3</sup> J. C. Hamilton, J. M. Blakely, Surf. Sci. **91**, 199 (1980).
  - <sup>4</sup> J. W. May, Surf. Sci. **17**, 267 (1969).
  - <sup>5</sup> K. S. Novoselov, A. K. Geim, S. V. Morozov, D. Jiang, Y. Zhang, S. V. Dubonos, I. V. Grigorieva, A. A. Firsov, Science **306**, 666 (2004).
  - <sup>6</sup> J. Wintterlin and M.-L. Bocquet, Surface Sci. **603**, 1841 (2009).
  - <sup>7</sup> C. Mattevi, Ho. Kim and M. Chhowalla, J. Mater. Chem., **21**, 3324 (2011).
  - <sup>8</sup> Y. S. Dedkov, M. Fonin, U. Rudiger, and C. Laubschat, Appl. Phys. Lett. **93**, 022509 (2008) ; Y. S. Dedkov, M. Fonin, and C. Laubschat, Appl. Phys. Lett. **92**, 052506 (2008).
  - <sup>9</sup> B. Borca, F. Calleja, J. J. Hinarejos, A. L. Vazquez de Parga and R. Miranda, J. Phys.: Condens. Matter **21** 134002 (2009).
  - <sup>10</sup> S. Gadipelli, I. Calizo, J. Ford, G. Cheng, A.R.H. Walker and T. Yildirim, J. Mater. Chem. **21**, 16057 (2011).
  - <sup>11</sup> S. Chen, L. Brown, M. Levendorf, W. Cai, Sang-Yong Ju, J. Edgeworth, X. Li, C. W. Magnuson, A. Velamakanni, R. D. Piner, J. Kang, J. Park, and R. S. Ruoff ACS Nano, **5** (2), 1321 (2011).
  - <sup>12</sup> J. Cho, L. Gao, J. Tian, H. Cao, W. Wu, Q. Yu, E. N. Yitamben, B. Fisher, J. R. Guest, Y. P. Chen, and N. P. Guisinger, ACS Nano **5** (5), 3607 (2011).
  - <sup>13</sup> N. A. Vinogradov, K. Schulte, M. L. Ng, A. Mikkelsen, E. Lundgren, N. Mrtensson, and A. B. Preobrajenski J. Phys. Chem. C, **115** (19), 9568 (2011).
  - <sup>14</sup> G. Kresse and J. Hafner, Phys. Rev. B **47**, 558 (1993).
  - <sup>15</sup> G. Kresse and J. Furthmüller, Phys. Rev. B **54**, 11169 (1996).
  - <sup>16</sup> J. P. Perdew, K. Burke, and M. Ernzerhof, Phys. Rev. Lett. **77**, 3865 (1996).
  - <sup>17</sup> S. Grimme, J. Comput. Chem. **27**, 1787 (2006).
  - <sup>18</sup> P. E. Blochl, Phys. Rev. B **50**, 17953 (1994).
  - <sup>19</sup> J.K. Grepstad, P.O. Gartland, B.J. Slagsvold: Surf. Sci. **57**, 348 (1976).
  - <sup>20</sup> G. Henkelman, A. Arnaldsson, and H. Jónsson, Comput. Mater. Sci. **36**, 254 (2006).
  - <sup>21</sup> Z. Wei, D. Wang, S. Kim, Soo-Young Kim, Y. Hu, M. K. Yakes, A. R. Laracuente, Z. Dai, S. R. Marder, C. Berger, W. P. King, W. A. de Heer, Paul E. Sheehan and Elisa Riedo, Science, **328** 1373 (2010).
  - <sup>22</sup> O. O. Ekiz, M. Urel, H. Guner, A. K. Mizrak, and A. Dana, ACS Nano, **5**, 2475 (2011).
  - <sup>23</sup> L. Signorini, L. Pasquini, L. Savini, R. Carboni, F. Boscherini, E. Bonetti, A. Giglia, M. Pedio, N. Mahne, and S. Nannarone, Phys. Rev. B **68**, 195423 (2003).
  - <sup>24</sup> I. P. Batra and S. Ciraci, Phys. Rev. B **29**, 6419 (1984).
  - <sup>25</sup> A. Kiejna, Phys. Rev. B **68**, 235405 (2003).
  - <sup>26</sup> P. Giannozzi, S. Baroni, N. Bonini, and thirty other coauthors, J. Phys. Condens. Matter **21**, 395502 (2009).
  - <sup>27</sup> M. Vanin, J. J. Mortensen, A. K. Kelkkanen, J. M. Garcia-Lastra, K. S. Thygesen, and K. W. Jacobsen, Phys. Rev. B **81**, 081408 (2010).
  - <sup>28</sup> A. Buldum, D.M. Leitner and S. Ciraci, Phys. Rev. B. **59**, 16042 (1999).
  - <sup>29</sup> H. Sevincli, S. Mukhopadhyay, R.T. Senger and S. Ciraci, Phys. Rev. B. **76**, 205430 (2007).
  - <sup>30</sup> M. Topsakal, E. Akturk, H. Sevincli and S. Ciraci, Phys. Rev. B. **78**, 235435 (2008).
  - <sup>31</sup> A. Hashimoto, K. Suenaga, A. Gloter, K. Urita, and S. Iijima, Nature (London) **430**, 870 (2004).
  - <sup>32</sup> S.M. Lee, Y.H. Lee, Y.G. Hwang, J.R. Hahn and H. Kang, Phys. Rev. Lett. **82**, 217 (1999).
  - <sup>33</sup> J.M. Carlsson, F. Hanke, S. Linic, and M. Scheffler, Phys. Rev. Lett. **102**, 166104 (2009).